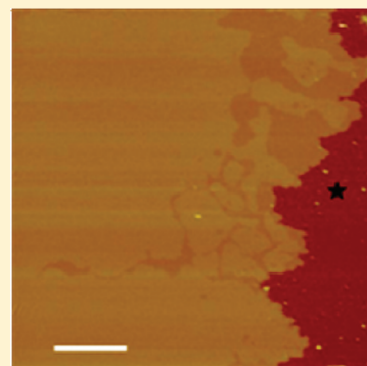


# Acyl Chain Differences in Phosphatidylethanolamine Determine Domain Formation and LacY Distribution in Biomimetic Model Membranes

Carne Suárez-Germà,<sup>†</sup> M.Teresa Montero,<sup>†</sup> Jordi Ignés-Mullol,<sup>‡</sup> Jordi Hernández-Borrell,<sup>\*,†</sup> and Òscar Domènech<sup>†</sup>

<sup>†</sup>Department of Physical Chemistry, Faculty of Pharmacy, and <sup>‡</sup>Faculty of Chemistry, IN<sup>2</sup>UB, University of Barcelona, E-08028-Barcelona, Spain

**ABSTRACT:** Phosphatidylethanolamine (PE) and phosphatidylglycerol (PG) are the two main components of the inner membrane of *Escherichia coli*. It is well-known that inner membrane contains phospholipids with a nearly constant polar headgroup composition. However, bacteria can regulate the degree of unsaturation of the acyl chains in order to adapt to different external stimuli. Studies on model membranes of mixtures of PE and PG, mimicking the proportions found in *E. coli*, can provide essential information on the phospholipid organization in biological membranes and may help in the understanding of membrane proteins activity, such as lactose permease (LacY) of *E. coli*. In this work we have studied how different phosphatidylethanolamines differing in acyl chain saturation influence the formation of laterally segregated domains. Three different phospholipid systems were studied: DOPE:POPG, POPE:POPG, and DPPE:POPG at molar ratios of 3:1. Lipid mixtures were analyzed at 24 and 37 °C through three different model membranes: monolayers, liposomes, and supported lipid bilayers (SLBs). Data from three different techniques, Langmuir isotherms, Laurdan generalized polarization, and atomic force microscopy (AFM), evidenced that only the DPPE:POPG system exhibited coexistence between gel ( $L_\beta$ ) and fluid ( $L_\alpha$ ) phases at both 24 and 37 °C. In the POPE:POPG system the  $L_\beta/L_\alpha$  coexistence appears at 27 °C. Therefore, in order to investigate the distribution of LacY among phospholipid phases, we have used AFM to explore the distribution of LacY in SLBs of the three phospholipid systems at 27 °C, where the DOPE:POPG is in  $L_\alpha$  phase and POPE:POPG and DPPE:POPG exhibit  $L_\beta/L_\alpha$  coexistence. The results demonstrate the preferential insertion of LacY in fluid phase.



## INTRODUCTION

Besides its high content in proteins, the inner lipid bilayer of *Escherichia coli* is composed of three main phospholipids: phosphatidylethanolamine (PE, zwitterionic, 74% of the total molar phospholipid content), phosphatidylglycerol (PG, bearing a negative charge, 19%), and cardiolipin (CL, bearing two negative charges, 3%).<sup>1</sup> Phospholipids, however, are not regarded anymore as a mere barrier but as components that exert strong influence over the activity and structure of membrane proteins.<sup>2–4</sup> Hence the investigation on interactions between lipids and specific proteins in biomembranes becomes of crucial interest for understanding physiological and pathological situations related to protein membrane activity.<sup>5</sup> As illustrated by the mechanosensitive channel proteins,<sup>6</sup> it is plausible to assume that basic physicochemical properties such as lateral compressibility, hydrophobic mismatch, or proton bridging capabilities of phospholipids surrounding transmembrane proteins may influence<sup>7</sup> or be part<sup>8</sup> of the transport phenomena. On the other hand, biomembranes are, as a whole, very dynamic structures where different assemblies occur, including lateral separation in domains<sup>9,10</sup> or selective segregation of particular species in the presence of membrane proteins.<sup>11</sup> Lateral heterogeneity is considered to play a major role in cell and developmental biology. It has been related

to signal transduction, cellular adhesion, protein folding and activation or membrane fusion.<sup>12,13</sup> In signal transduction processes, for instance, it is crucial to understand how protein receptors in the surface of the cell adopt their tertiary structures. In this particular field the earlier works of Khorana's group on photoreceptors become illustrative.<sup>14,15</sup> In general, however, there are at the present few doubts on the influence of membrane lipids on the structure and organization of membrane proteins.<sup>16</sup>

In these regards, we have shown, on one hand, that on the basis of FRET measurements in proteoliposomes of mixed 1-palmitoyl-2-oleoyl-*sn*-glycero-3-phosphoglycerol (POPG) and PEs differing in the saturation degree of the acyl chains, lactose permease (LacY) of *E. coli*, a paradigm for the secondary transport,<sup>5,17</sup> prefers PE instead of PG in the annular region.<sup>18,19</sup> On the other hand, using the binary mixture of POPG with 1-palmitoyl-2-oleoyl-*sn*-glycero-3-phosphoethanolamine (POPE), atomic force microscopy (AFM) observations of supported lipid bilayers (SLBs) evidenced that LacY inserts preferentially into the fluid phase ( $L_\alpha$ ) instead of inserting into the gel phase ( $L_\beta$ ).<sup>20</sup>

**Received:** July 6, 2011

**Revised:** September 27, 2011

**Published:** September 30, 2011

However, naturally occurring phospholipids found under physiological conditions feature mixed acyl chains, one saturated (at the *sn*-1 position) and the other unsaturated (at the *sn*-2 position) linked to the glycerol backbone. While the PE/PG ratio may remain nearly constant upon different situations, bacteria can regulate the composition and the degree of unsaturation of the acyl chains to adapt to different external stimuli.<sup>21</sup> As a result, phase separation may occur, which will affect lateral distribution of transmembrane proteins<sup>22</sup> and induce changes in lipid composition in the annular region.<sup>11,18,19</sup> Therefore, it becomes relevant to investigate and compare whether binary mixtures of PG and PE with different acyl composition form laterally segregated domains in monolayers, liposomes, and SLBs.

In this work, we have investigated the mixing properties of the binary mixtures of POPG with either the heteroacid POPE or the saturated homoacid 1,2-palmitoyl-*sn*-glycero-3-phosphoethanolamine (DPPE), or the unsaturated homoacid 1,2-oleoyl-*sn*-glycero-3-phosphoethanolamine (DOPE). The characterization of these systems in monolayers, liposomes, and SLBs may provide means to understand the interaction and specific selectivity between phospholipid species and membrane proteins. Thereafter we have investigated the distribution of LacY in these systems.

## EXPERIMENTAL METHODS

1,2-Palmitoyl-*sn*-glycero-3-phosphoethanolamine (DPPE), 1,2-oleoyl-*sn*-glycero-3-phosphoethanolamine (DOPE), 1-palmitoyl-2-oleoyl-*sn*-glycero-3-phosphoethanolamine (POPE), and 1-palmitoyl-2-oleoyl-*sn*-glycero-3-[phospho-rac-(1-glycerol)] (sodium salt) (POPG) were purchased from Avanti Polar Lipids (Alabaster, AL). Laurdan (6-dodecanoyl-2-dimethyl-aminonaphthalene) was purchased from Molecular Probes (Invitrogen, Carlsbad, CA). All other common chemicals, ACS grade, were purchased from Sigma (St. Louis, MO). Buffer used throughout the experiments was 20 mM HEPES (pH 7.40) and 150 mM NaCl prepared in ultrapure water (Milli-Q reverse osmosis system, 18.2 MΩ cm resistivity). For SLB formation, the buffer was supplemented with 10 mM CaCl<sub>2</sub>. Lactose permease (LacY) was obtained from bacterial culture, extracted, and purified according to procedures described elsewhere.<sup>18–20</sup>

**Surface Pressure–Area Isotherms.** Monolayers differing on lipid composition were prepared in a 312 DMC Langmuir–Blodgett trough manufactured by NIMA Technology Ltd. (Coventry, England). The trough (total area, 137 cm<sup>2</sup>) was placed on a vibration-isolated table (Newport, Irvine, CA) and enclosed in an environmental chamber. The resolution of the surface pressure measurement was ±0.1 mN m<sup>−1</sup>. Temperature was maintained via an external circulating water bath (±0.2 °C). Before each experiment, the trough was washed with ethanol and rinsed thoroughly with purified water.

Experiments were performed as described in a previous paper.<sup>23</sup> The corresponding aliquot of chloroform–methanol (2:1, v/v) lipid solution was spread onto the subphase with a Hamilton microsyringe. A 15 min period was required for solvent to evaporate before each experiment. The compression barrier speed was 5 cm<sup>2</sup> min<sup>−1</sup>. Every surface pressure–area ( $\pi$ – $A$ ) isotherm was repeated three times minimum, with the isotherms showing satisfactory reproducibility.

Surface thermodynamic analysis of the mixed monolayers at 30 mN m<sup>−1</sup> was done in order to analyze miscibility and interactions between their components. The interaction between two phospholipid components in a mixed monolayer, at a constant

surface pressure  $\pi$  and temperature, can be evaluated from the calculation of the excess Gibbs energy ( $G^E$ ), which is given by

$$G^E = \int_0^\pi [A_{12} - \chi_1 A_1 - \chi_2 A_2] d\pi \quad (1)$$

where  $A_{12}$  is the average area per molecule of the mixed monolayer at a given pressure,  $A_1$  and  $A_2$  are the area per molecule of the pure components at this pressure, and  $\chi_1$  and  $\chi_2$  are the mole fractions of each component.

Stability of the mixed monolayers was verified by computing the values of the Gibbs energy of mixing ( $\Delta_{\text{mix}}G$ ),

$$\Delta_{\text{mix}}G = \Delta_{\text{mix}}G^{\text{id}} + G^E \quad (2)$$

where the first term, the ideal Gibbs energy of mixing ( $\Delta_{\text{mix}}G^{\text{id}}$ ), is given by

$$\Delta_{\text{mix}}G^{\text{id}} = RT(\chi_1 \ln \chi_1 + \chi_2 \ln \chi_2) \quad (3)$$

where  $R$  is the universal gas constant and  $T$  is the temperature.

The inverse of the isothermal compressibility or elastic modulus of area compressibility ( $C_s^{-1}$ ) was calculated using

$$C_s^{-1} = (-A) \left( \frac{\partial \pi}{\partial A} \right)_{T,n} \quad (4)$$

The derivative of the experimental data was computed by fitting a straight line to a window of area width of 0.2 nm<sup>2</sup> molec<sup>−1</sup> around any given surface pressure value, so that experimental noise was filtered out.

**Large Unilamellar Vesicle Formation.** Liposomes of DOPE:POPG (3:1, mol/mol), POPE:POPG (3:1, mol/mol), and DPPE:POPG (3:1, mol/mol) were prepared according to methods previously described.<sup>18,19</sup> Chloroform–methanol (2:1, v/v) solutions containing appropriate amounts of each phospholipid were dried under a stream of oxygen-free N<sub>2</sub> in a conical tube. The resulting thin film was kept under high vacuum for approximately 3 h to remove organic solvent traces. Multilamellar liposomes (MLVs) were formed by redispersing the films with the above-mentioned buffer, applying successive cycles of freezing and thawing below and above the phase transition of the phospholipids, and vortexing for 2 min. Finally, large unilamellar vesicles (LUVs) were obtained by extrusion of the MLVs through 100 nm pore polycarbonate filters (Mini-extruder, Avanti, and Nucleopore filters).

**Fluorescence Measurements.** Bilayer fluidity was monitored using dipolar relaxation of Laurdan. Briefly, Laurdan is a polarity sensitive probe that tends to locate at the glycerol backbone of the bilayer with the lauric acid tail anchored in the phospholipid acyl chain region.<sup>24</sup> Upon excitation, the dipole moment of Laurdan increases noticeably, and water molecules in the vicinity of the probe reorient around this new dipole. When the membrane is in a fluid phase, the reorientation rate is faster than the emission process, and consequently, a red-shift is observed in the emission spectrum of Laurdan. When the bilayer packing increases, part of the water molecules is excluded from the bilayer and the dipolar relaxation of the remaining water molecules is slower, leading to a fluorescent spectrum that is significantly less shifted to the red.<sup>25</sup>

We monitored the bilayer fluidity-dependent fluorescence spectral shift of Laurdan due to dipolar relaxation phenomena. Determinations were carried out using an SLM-Aminco 8100 spectrofluorimeter equipped with a jacketed cuvette holder. The temperature (±0.2 °C) was controlled using a circulating bath

(Haake K20, Germany). The excitation and emission slits were 4 and 4 nm and 8 and 8 nm, respectively. The lipid concentration in the liposome suspension was adjusted to 250  $\mu\text{M}$ , and Laurdan was added to give a lipid/probe ratio of 300. Generalized polarization ( $\text{GP}_{\text{ex}}$ ) from emission spectra was calculated using

$$\text{GP}_{\text{ex}} = \frac{I_{440} - I_{490}}{I_{440} + I_{490}} \quad (5)$$

where  $I_{440}$  and  $I_{490}$  are the fluorescence intensities at emission wavelengths of 440 nm (gel phase,  $L_{\beta}$ ) and 490 nm (liquid crystalline phase,  $L_{\alpha}$ ), respectively.

$\text{GP}_{\text{ex}}$  values as a function of temperature were fitted to a Boltzmann-like equation

$$\text{GP}_{\text{ex}} = \text{GP}_{\text{ex}}^2 + \frac{\text{GP}_{\text{ex}}^1 - \text{GP}_{\text{ex}}^2}{1 + \exp\left\{\frac{T_m - T}{m}\right\}} \quad (6)$$

where  $\text{GP}_{\text{ex}}^1$  and  $\text{GP}_{\text{ex}}^2$  are the maximum and minimum values of  $\text{GP}_{\text{ex}}$ ,  $T_m$  is the gel to fluid phase transition temperature of the studied composition,  $T$  is the temperature, and  $m$  is the slope of the transition that gives information about the cooperativity of the process.

**Supported Lipid Bilayers and Atomic Force Microscopy.** The spread of the SLBs was obtained by using the vesicle fusion technique as described elsewhere.<sup>26</sup> Briefly, 80  $\mu\text{L}$  of LUVs, in 20 mM Hepes pH 7.40, 150 mM NaCl, and 10 mM  $\text{CaCl}_2$  buffer, were deposited onto freshly cleaved mica disks mounted on a Teflon O-ring. Samples were incubated at 50  $^{\circ}\text{C}$  for 2 h in an oven preventing the water evaporation from the sample using a water reservoir, before being washed with 10 mM Hepes pH 7.40, 150 mM NaCl. Proteoliposomes (at a lipid to protein ratio of 40) were prepared following the same protocol, but incubation did not exceed 37  $^{\circ}\text{C}$ . The tip was immediately immersed into the liquid cell. To perform all these experiments it was necessary to drift equilibrate and thermally stabilize the cantilever for 30 min in the presence of buffer.

Liquid AFM imaging was performed using a Multimode Microscope controlled by a Nanoscope V electronics (Digital Instruments, Santa Barbara, CA), in tapping mode acquisition (TM-AFM) at minimum vertical force, maximizing the amplitude set point value and maintaining the vibration amplitude as low as possible. V-shaped  $\text{Si}_3\text{N}_4$  cantilevers (MLCT-AUNM, Veeco) with a nominal spring constant of 0.10  $\text{N m}^{-1}$  were used. Variable temperature experiments were performed by incorporating a temperature controller stage (Digital Instruments, Santa Barbara, CA) to the piezo-scanner. This device allows the maintenance of the sample holder at a fixed temperature (range, from room temperature up to 62.5  $^{\circ}\text{C}$ ; resolution, 0.1  $^{\circ}\text{C}$ ; temperature drift, <0.5  $^{\circ}\text{C}$ ).

## RESULTS AND DISCUSSION

Lipid monolayers constitute a convenient model system to investigate the interactions and physicochemical properties of phospholipids forming biological membranes. Thus, lateral pressure in biomembranes has been postulated as a mechanism for modulation of transmembrane protein function.<sup>27,28</sup> For this reason we have used Langmuir monolayers to investigate intermolecular interactions between the major phospholipid components, PE and PG, of the inner *E. coli* membrane.<sup>1</sup> In particular these experiments have been delineated to gather information on

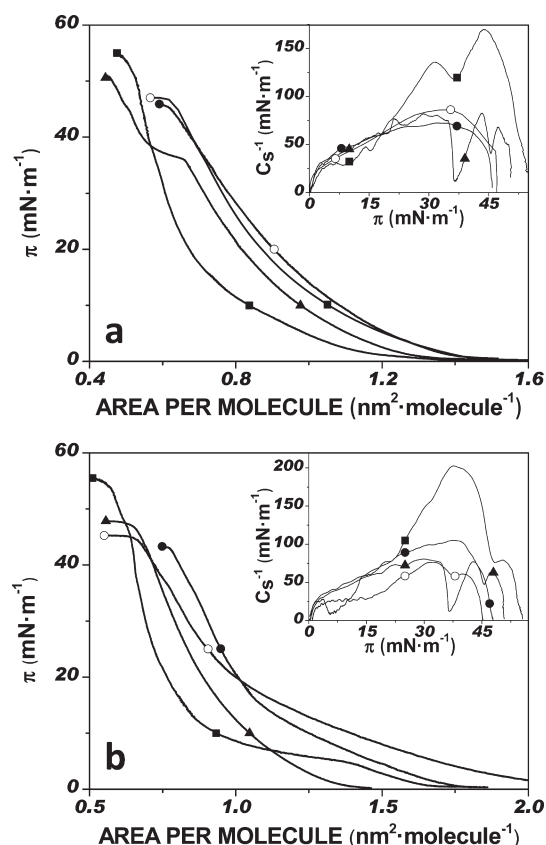


**Figure 1.** Surface pressure–area isotherms of pure DPPE (■), POPE (▲), POPG (○), and DOPE (●) at (a) 24  $^{\circ}\text{C}$  and (b) 37  $^{\circ}\text{C}$ . Insets show the elastic moduli of area compressibility ( $C_s^{-1}$ ) corresponding to each isotherm.

the structural relevance of the saturation degree of the acyl chains of PE.

The surface pressure–area ( $\pi$ – $A$ ) compression isotherms of the pure phospholipids at 24 and 37  $^{\circ}\text{C}$  are shown in Figure 1 along with  $C_s^{-1}$  values (insets). As expected, PE monolayers show higher area per molecule the more unsaturated hydrocarbon chains they contain. These data emphasize the fact that acyl chains play a predominant role in the overall packing of the monolayer which is determined by the degree of unsaturation of the acyl chains. Thus, the existence of a C–C double bond leads to the formation of a kink, producing chain shortening. Besides, it also generates higher intermolecular steric effects increasing the distances between individual molecules. The effect is at the maximum when both acyl chains are unsaturated. This can be observed in Figure 1 where DOPE shows the largest monolayer intermolecular distances. Conversely, DPPE, with both acyl chains saturated, remains as the more compressed molecule. An intermediate situation was found for POPE. These monolayer features are consistent with results found in the literature.<sup>29–32</sup> As discussed by Wydro and Witkowska,<sup>29</sup> while a DPPE monolayer at 24  $^{\circ}\text{C}$  features a liquid expanded (LE) to solid (S) phase transition at  $\sim 37 \text{ mN m}^{-1}$ , DOPE is always in the LE phase. These behaviors are consistent with the values of the compression modulus shown in the inset of Figure 1. The POPE isotherm shows, in turn, the characteristic LE–LC phase transition at  $\sim 36 \text{ mN m}^{-1}$  whose nanostructure and characteristics have been previously discussed.<sup>33</sup> It is known that POPG is always in the



LE phase above 20 °C.<sup>34,35</sup> Thus, at 37 °C POPE and DOPE monolayers are in the LE phase while DPPE shows a LE–LC phase transition at  $\sim 4.7$  mN m<sup>−1</sup>. When comparing PE and PG headgroups with the same hydrocarbon chain, PE shows at 24 and 37 °C higher areas per molecule at surface pressures below 40 mN m<sup>−1</sup>. This is attributable to the negative charge born by the PG headgroups and to the size of each headgroup. Besides, both PE amino and PG hydroxyl headgroups are able to form intermolecular hydrogen bonds at physiological pH conditions.<sup>36</sup> However, PG–PG interactions are weaker than those arising between PE zwitterions. Indeed, it is known that PE headgroups tightly interact, creating a hydrogen bond network which confers rigidity to the monolayer.<sup>23</sup>

Lipid mixtures DPPE:POPG, POPE:POPG, and DOPE:POPG (3:1, mol/mol) were also studied using Langmuir monolayers. For these mixed systems,  $\pi$ –A compression isotherms are shown in Figure 2 along with the  $C_s^{-1}$  values (insets). The addition of POPG to the pure PE lipids led to remarkable changes in the features of all isotherms. At a surface pressure

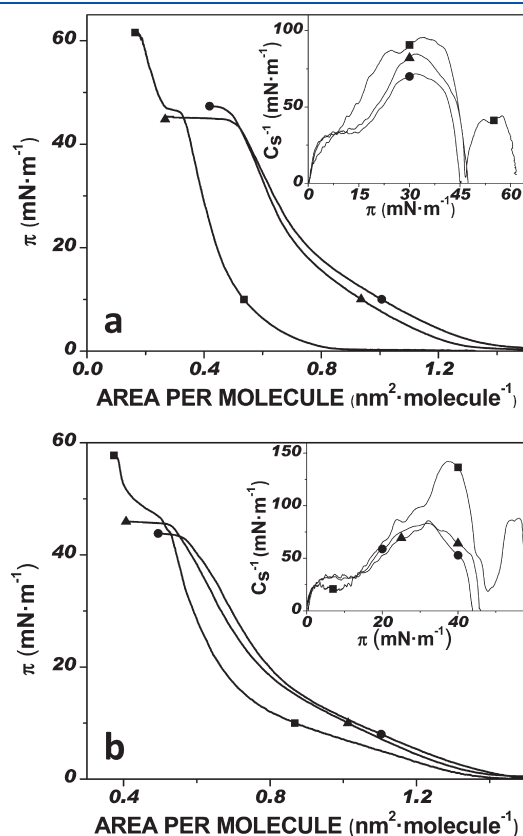


**Figure 2.** Surface pressure–area isotherms of DPPE:POPG (3:1, mol/mol) (■), POPE:POPG (3:1, mol/mol) (▲), and DOPE:POPG (3:1, mol/mol) (●) at (a) 24 °C and (b) 37 °C. Insets show the elastic moduli of area compressibility ( $C_s^{-1}$ ) corresponding to each isotherm.

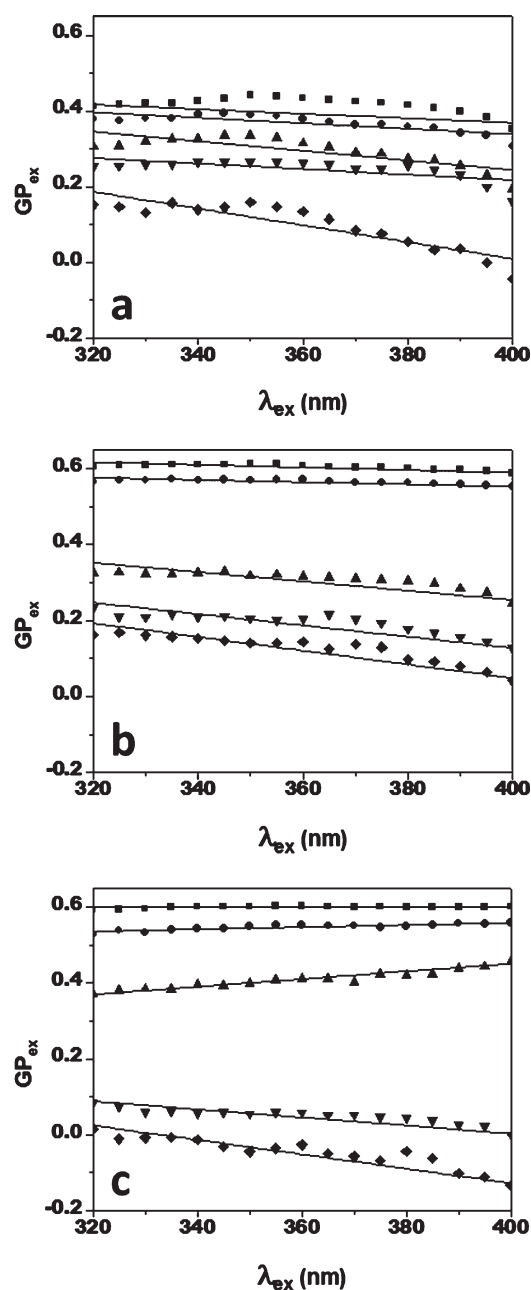
of 30 mN m<sup>−1</sup>, a pressure considered as representative for a bilayer,<sup>28</sup> all the mixed monolayers showed lower area per molecule than their corresponding pure phospholipid components. As expected, these monolayers showed again higher area per molecule as the number of double bonds of PE increased. It is also worth mentioning the special case of the DPPE:POPG isotherm shown in Figure 2, where two transitions occur at both studied temperatures. Well-defined collapse pressures and characteristic plateaus were observed at 61 and 46 mN m<sup>−1</sup>, at 24 °C, and 58 and 43 mN m<sup>−1</sup>, at 37 °C, respectively. This behavior can be more precisely observed by analyzing the  $C_s^{-1}$  values plotted in the insets of Figure 2. Since the pressures at which these features occur do not coincide with the collapse pressure of the pure components, the existence of pure DPPE and POPG domains can be excluded. Most likely these observations are evidence of the lateral segregation in two different lipid domains, both enriched in one of the components.

In Table 1 the values of  $C_s^{-1}$ ,  $G^E$ , and  $\Delta_{\text{mix}}G$  calculated at 30 mN m<sup>−1</sup> are listed. The low negative deviations of these values observed for POPE:POPG and DOPE:POPG indicate the existence of attractive interactions and confirm the stability of these systems. Conversely, positive and larger values of  $G^E$  are found at both temperatures in the DPPE:POPG mixture which is strong evidence of repulsive interactions between both components. This may result in partial miscibility of the components and in their organization in phase separation. Concerning miscibility studies, we have proved by AFM that there is a clear influence between the phase separation in monolayers and the domains observed in bilayers blistered by double deposition of monolayers.<sup>37</sup> Hence, it becomes relevant to investigate the existence of phase separation in the bilayers formed with the same phospholipids used in the monolayer study. To further characterize the specific behavior of the mixed systems, liposomes were used to investigate possible phase separation and also to establish  $T_m$  by exploiting Laurdan fluorescence properties. Thus, changes in fluorescence intensity of the probe as a function of temperature and excitation wavelength ( $\lambda_{\text{ex}}$ ) in the range of temperatures from 3 to 65 °C were studied. As it can be seen in Figure 3, DOPE:POPG (3:1, mol/mol) lipid mixture was found in  $L_\alpha$  phase throughout the range of temperatures used in the experiment. However the  $T_m$  of this system could not be established due to technical limitations because both pure DOPE and pure POPG have nominal  $T_m$  values below 0 °C.

On one hand, the  $T_m$  for the mixtures of POPE:POPG (3:1, mol/mol) and DPPE:POPG (3:1, mol/mol) were established at 23.3 and 51.1 °C. Below and above these temperatures  $L_\beta$  and  $L_\alpha$  phases are observed, respectively. On the other hand the mixture DPPE:POPG (3:1, mol/mol) was the only studied system showing positive slopes between single  $L_\beta$  and  $L_\alpha$  phases. Positive slopes indicate coexistence of  $L_\beta$  and  $L_\alpha$  phases. They were observed ranging from 21.3 °C (data not shown) to 49.0 °C, indicating the coexistence of two phases in this range of temperatures. This finding is consistent with the information

**Table 1.** Mathematical Analysis of the Surface Pressure–Area Isotherms from Figure 2

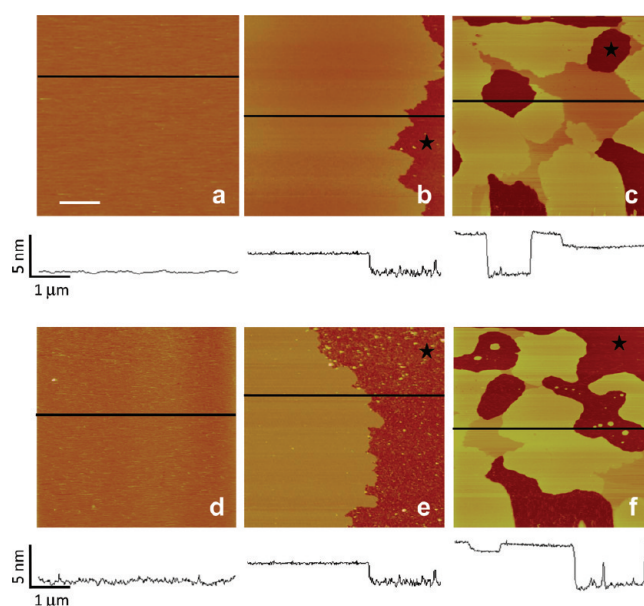
composition (3:1, mol/mol)	24 °C			37 °C		
	$C_s^{-1}$ (mN m <sup>−1</sup> )	$G^E$ (kJ mol <sup>−1</sup> )	$\Delta_{\text{mix}}G$ (kJ mol <sup>−1</sup> )	$C_s^{-1}$ (mN m <sup>−1</sup> )	$G^E$ (kJ mol <sup>−1</sup> )	$\Delta_{\text{mix}}G$ (kJ mol <sup>−1</sup> )
DPPE:POPG	91	1.35	−0.04	99	1.30	−0.14
POPE:POPG	82	−0.53	−1.92	81	−0.07	−1.52
DOPE:POPG	70	−0.85	−2.24	77	0.99	−0.45



**Figure 3.**  $GP_{ex}$  as a function of  $\lambda_{ex}$  for (a) DOPE:POPG (3:1, mol/mol) ( $\blacksquare$  = 3.2 °C,  $\bullet$  = 8.0 °C,  $\blacktriangle$  = 18 °C,  $\blacktriangledown$  = 26.5 °C, triangle pointing left = 38.9 °C), (b) POPE:POPG (3:1, mol/mol) ( $\blacksquare$  = 2.7 °C,  $\bullet$  = 16.4 °C,  $\blacktriangle$  = 24.3 °C,  $\blacktriangledown$  = 32.7 °C,  $\blacklozenge$  = 41.0 °C), and (c) DPPE:POPG (3:1, mol/mol) ( $\blacksquare$  = 10.7 °C,  $\bullet$  = 23.8 °C,  $\blacktriangle$  = 43.0 °C,  $\blacktriangledown$  = 56.0 °C,  $\blacklozenge$  = 64.6 °C).

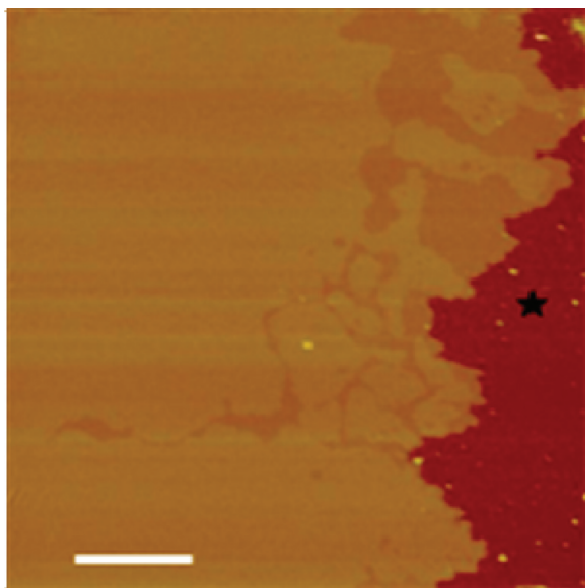
obtained from the compression isotherms that suggest phase separation.

Figure 4 shows the AFM characterization at 24 and 37 °C of SLBs of the different phospholipid systems. On one hand, the topographic images shown in Figure 4a,d, corresponding to SLBs obtained by extension of DOPE:POPG (3:1, mol/mol) liposomes, feature a homogeneous layer. According to the nominal  $T_m$  of both phospholipids, these layers correspond to SLBs in  $L_\alpha$  phase. The layer thickness, however, could not be inferred from line profile analysis because of complete coverage of the mica



**Figure 4.** Topography AFM images of SLBs at 24 °C: (a) DOPE:POPG (3:1, mol/mol), (b) POPE:POPG (3:1, mol/mol), and (c) DPPE:POPG (3:1, mol/mol). At 37 °C: (d) DOPE:POPG (3:1, mol/mol), (e) POPE:POPG (3:1, mol/mol), and (f) DPPE:POPG (3:1, mol/mol). Black star indicates mica substrate. Scale bar = 1  $\mu$ m. Z scale = 20 nm.

substrate and absence of defects. Similar features are observed in Figure 4b, where the SLBs of POPE:POPG at 24 and 37 °C exhibited also a homogeneous layer. Taking the substrate as reference, the thickness of the POPE:POPG bilayer (3:1, mol/mol) could be established in  $3.4 \pm 0.3$  nm ( $n = 50$ ) and  $3.0 \pm 0.3$  nm ( $n = 50$ ) at 24 and 37 °C, respectively. These values are slightly lower than others previously obtained for the same system,<sup>26</sup> which could be attributed to the absence of calcium in the present experiments. Additionally, in that work it has been demonstrated by DSC that the POPE:POPG system undergoes a  $L_\beta$  to  $L_\alpha$  transition at 21 °C, which coincides with the value found from our  $GP_{ex}$  experiments (see above). It is noteworthy that because of the presence of the mica substrate SLBs feature two decoupled phase transitions. Thus, the value of  $T_m$  obtained from DSC of liposomes is interpreted as the representative for the melting of the proximal leaflet in SLBs. Indeed in SLBs this value is shifted to higher temperatures.<sup>38</sup> A detailed investigation of the thermal response of POPE:POPG SLBs under different conditions has been published by Seeger and co-workers.<sup>39</sup> In good comparison with the observations of these authors and in agreement with our previously reported observations, two laterally segregated domains for the POPE:POPG system at 27 °C can be seen in Figure 5.<sup>37</sup> On the other hand, laterally segregated domains for the SLBs of DPPE:POPG (3:1, mol/mol) are observed, that according to Laurdan experiments should be assigned to segregated  $L_\beta$  and  $L_\alpha$  phases. The characteristic thicknesses, taking mica as a reference for the line profile analysis, were  $5.7 \pm 0.3$  nm and  $7.6 \pm 0.3$  nm for the thinner and thicker lipid domains at 24 °C, and  $5.8 \pm 0.3$  nm and  $7.2 \pm 0.3$  nm at 37 °C, respectively. These values are higher than expected in comparison with the heights obtained for POPE:POPG. Since the values for pure DPPE bilayers found in literature are  $\sim 5.4$  nm,<sup>40</sup> the formation of multilayers should be somehow excluded. Most likely the discrepancies would arise because of other factors as the



**Figure 5.** Topography AFM images of POPE:POPG (3:1, mol/mol) at 27 °C. Black star indicates mica substrate. Scale bar = 1  $\mu\text{m}$ . Z scale = 20 nm.

force applied or a possible repulsion between the tip and the  $L_\beta$  phase in the DPPE:POPG system.<sup>26</sup> At this point further discussion is not possible without knowing the exact composition of the domains.

There is a general consensus on the matching between the hydrophobic thickness of the phospholipid bilayer and the transmembrane segments of the protein membranes. This theoretical concept<sup>41</sup> has received experimental support for LacY<sup>42</sup> or melibiose permease (MelB) of *E. coli*.<sup>43</sup> The seminal work based on the use of pyrene-labeled lipids, which are able to form excimers, suggested the enrichment of phospholipids according to this matching principle.<sup>41</sup> However, posterior works based on FRET between a single tryptophan mutant of LacY and pyrene-labeled phospholipids have shown that LacY is able to perform a molecular sorting by recruiting the most abundant lipid in binary mixtures of PE and PG.<sup>18</sup> Importantly, this matching principle is sustained by our data since the thickness of the bilayers, as measured by AFM (see profile analysis in Figure 4), matches well with the estimated hydrophobic thickness of LacY.<sup>17</sup>

Otherwise, it becomes relevant to investigate how the phospholipid composition studied here influences LacY distribution. Indeed, the partitioning of LacY into  $L_\alpha$  phases was suggested in earlier works<sup>44</sup> where high concentrations of protein (lipid to protein ratio = 0.5) were used. Here, we have extended these observations to samples prepared at high lipid to protein ratios (less proportion of protein). Thus, when LacY is reconstituted in proteoliposomes of the same composition as the SLBs and observed with AFM at 27 °C, thicker structures protruding from the phospholipid matrices can be distinguished (Figure 6). These entities, most likely ascribable to LacY, protrude  $0.8 \pm 0.3$ ,  $1.4 \pm 0.5$ , and  $2.0 \pm 0.7$  nm from the SLBs of DOPE:POPG (3:1, mol/mol), POPE:POPG (3:1, mol/mol), and DPPE:POPG (3:1, mol/mol), respectively. Although the statistics is short ( $n = 30$ ), the fact that the protein protrudes more the less saturated the acyl chain species is may be a consequence of different lateral pressure exerted by each phospholipid.<sup>45</sup> Remarkably, these experiments demonstrate that, at lipid to protein ratios compatible with former

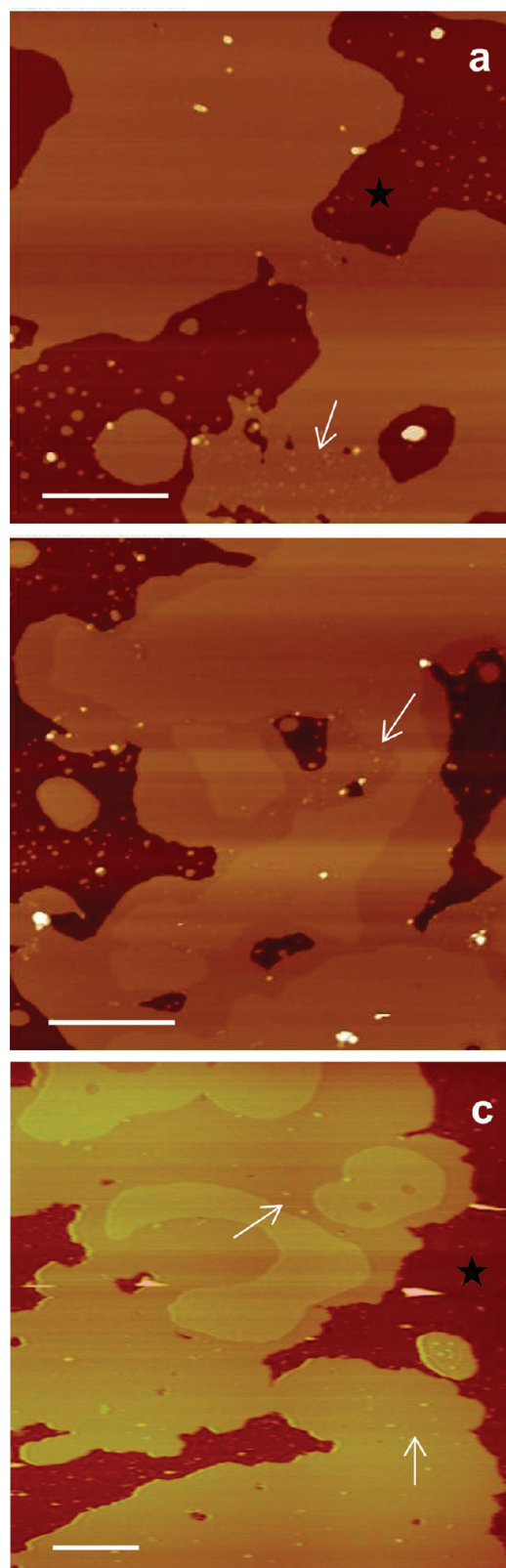


**Figure 6.** Topography AFM image of extended proteoliposomes of LacY (1.5  $\mu\text{M}$ ) at 27 °C: (a) DOPE:POPG (3:1, mol/mol), (b) POPE:POPG (3:1, mol/mol), and (c) DPPE:POPG (3:1, mol/mol). Black star indicates mica substrate. Arrows point to protrusions attributed to the presence of LacY. Scale bar = 500 nm. Z scale = 20 nm.



FRET experiments,<sup>18,19</sup> LacY prefers the  $L_{\alpha}$  phase. This coincides with a general behavior for protein membranes<sup>22</sup> and, remarkably, with the  $K^{+}$  ion channel (KcsA).<sup>46</sup> As can be seen in Figure 6b,c this preference has been clearly demonstrated here in the systems that form separated phases, that is POPE:POPG and DPPE:POPG.

Indeed, by using FRET tools we have previously shown<sup>18,19</sup> that PG is completely excluded from the annular region in the POPE:POPG system, only partially excluded from the DOPE:POPG matrix, and, conversely, segregated in PG enriched domains in the DPPE:POPG mixture. Results presented in this paper provide support for these interpretations.

## CONCLUSIONS

By studying the phase separated mixture of PE and PG, we demonstrate that LacY partitions into fluid phases. Even in the absence of phase diagrams for each binary mixture our results suggest that the fluid phases are enriched in POPG. This is not, however, in contradiction with the fact that LacY shows higher selectivity for PE than PG,<sup>47</sup> providing means for a protein-promoted membrane domain,<sup>11</sup> characterized by a lipid annulus mainly formed by PE.

## AUTHOR INFORMATION

### Corresponding Author

\*E-mail: jordihernandezborrell@ub.edu. Fax: (+34) 934035987. Phone: (+34) 934035986.

## ACKNOWLEDGMENT

C.S.-G. is recipient of a FPI fellowship from the Ministerio de Ciencia e Innovación of Spain. This work has been supported by Grant CTQ-2008-03922/BQU from Ministerio de Ciencia e Innovación of Spain.

## REFERENCES

- (1) Dowhan, W. *Annu. Rev. Biochem.* **1997**, *66*, 199.
- (2) Hakizimana, P.; Masureel, M.; Gbaguidi, B.; Ruysschaert, J. M.; Govaerts, C. *J. Biol. Chem.* **2008**, *283*, 9369.
- (3) Bogdanov, M.; Mileykovskaya, E.; Dowhan, W. *Subcell. Biochem.* **2008**, *49*, 197.
- (4) Schmidt, D.; Jiang, Q. X.; MacKinnon, R. *Nature* **2006**, *444*, 775.
- (5) Guan, L.; Kaback, H. R. *Ann. Rev. Biophys. Biomed. Struct.* **2006**, *35*, 67.
- (6) Wiggins, P.; Phipps, R. *Biophys. J.* **2005**, *2*, 880.
- (7) Dowhan, W.; Mileykovskaya, E.; Bogdanov, M. *Biochim. Biophys. Acta* **2004**, *1666*, 19.
- (8) Haines, T. H.; Dencher, N. A. *FEBS Lett.* **2002**, *528*, 35.
- (9) Jacobson, K.; Mouritsen, O. G.; Anderson, R. G. W. *Nat. Cell Biol.* **2007**, *9*, 1, 7.
- (10) Shultz, Z. D.; Levin, I. W. *Biophys. J.* **2008**, *94*, 3104.
- (11) Poveda, J. A.; Fernández, A. M.; Encinar, J. A.; González-Ros, J. M. *Biochim. Biophys. Acta* **2008**, *1778*, 1583.
- (12) Brown, D. A.; London, E. *Ann. Rev. Cell. Dev. Biol.* **1998**, *14*, 111.
- (13) Simons, K.; Gerl, M. J. *Nat. Rev. Mol. Cell. Biol.* **2010**, *11*, 688.
- (14) Ridge, K. D.; Bhattacharya, S.; Nakayama, T. A.; Khorana, H. G. *J. Biol. Chem.* **1992**, *267*, 6770.
- (15) Bhattacharya, S.; Ridge, K. D.; Knox, B. E.; Khorana, H. G. *J. Biol. Chem.* **1992**, *267*, 6763.
- (16) Nyholm, T. K.; Ozdirekcan, S.; Killian, J. A. *Biochemistry* **2007**, *46*, 1457.
- (17) Abramson, J.; Iwata, S.; Kaback, H. R. *Mol. Membr. Biol.* **2004**, *21*, 227.
- (18) Picas, L.; Montero, M. T.; Morros, A.; Vázquez-Ibar, J. L.; Hernández-Borrell, J. *Biochim. Biophys. Acta* **2010**, *1798*, 291.
- (19) Picas, L.; Suárez-Germà, C.; Montero, M. T.; Vázquez-Ibar, J. L.; Hernández-Borrell, J. *Biochim. Biophys. Acta* **2010**, *1798*, 1707.
- (20) Picas, L.; Carretero-Genevri, A.; Montero, M. T.; Vázquez-Ibar, J. L.; Seantier, B.; Milhiet, P. E.; Hernández-Borrell, J. *Biochim. Biophys. Acta* **2010**, *1798*, 1014.
- (21) Morein, S.; Andersson, A. S.; Råfors, L.; Lindblom, G. *J. Biol. Chem.* **1996**, *271*, 6801.
- (22) Houslay, M. D.; Stanley, K. K. *Dynamics of Biological Membranes*; Wiley & Sons: New York, 1982; p 116.
- (23) Domènech, O.; Sanz, F.; Montero, M. T.; Hernández-Borrell, J. *Biochim. Biophys. Acta* **2006**, *1758*, 213.
- (24) Parassassi, T.; Kransnowska, E. K.; Bagatolli, L.; Gratton, E. *J. Fluoresc.* **1998**, *8*, 365.
- (25) Domènech, O.; Dufrene, Y.; Van Bambeke, F.; Tulkens, P. M.; Mingeot-Leclercq, M. P. *Biochim. Biophys. Acta* **2006**, *1758*, 213.
- (26) Picas, L.; Montero, M. T.; Morros, A.; Cabañas, M. E.; Seantier, B.; Milhiet, P. E.; Hernández-Borrell, J. *J. Phys. Chem. B* **2009**, *112*, 4646.
- (27) Cantor, R. S. *J. Phys. Chem. B* **1997**, *101*, 1723.
- (28) Marsh, D. *Biochim. Biophys. Acta* **1996**, *1285*, 183.
- (29) Wydro, P.; Witkowska, K. *Colloids Surf., B* **2009**, *72*, 32.
- (30) Wydro, P.; Hac-Wydro, K. *J. Phys. Chem. B* **2007**, *111*, 2495.
- (31) Saulnier, P.; Foussard, F.; Boury, F.; Proust, J. E. *J. Colloid Interface Sci.* **1989**, *218*, 40.
- (32) Brockmann, H. L.; Applegate, K. R.; Momsem, M. M.; King, W. C.; Glomset, J. A. *Biophys. J.* **2003**, *85*, 2384.
- (33) Domènech, O.; Ignés-Mullol, J.; Montero, M. T.; Hernández-Borrell, J. *J. Phys. Chem. B* **2007**, *111*, 10946.
- (34) Takamoto, D. Y.; Lipp, M. M.; Von Nahmen, A.; Lee, K. Y. C.; Warning, A. J.; Zasadzinski, J. A. *Biophys. J.* **2001**, *81*, 153.
- (35) Sánchez-Martín, M. J.; Haro, I.; Alsina, M. A.; Busquets, M. A.; Pujol, M. *J. Phys. Chem. B* **2010**, *114*, 448.
- (36) Langmer, M.; Kubica, K. *Chem. Phys. Lipids* **1993**, *102*, 3.
- (37) Picas, L.; Suárez-Germà, C.; Montero, M. T.; Hernández-Borrell, J. *J. Phys. Chem. B* **2010**, *114*, 3543.
- (38) Keller, D.; Larsen, N. B.; Moller, I. M.; Mouritsen, O. G. *Phys. Rev. Lett.* **2005**, *94*, 025701.
- (39) Seeger, H. M.; Marino, G.; Alessandrini, A.; Facci, P. *Biophys. J.* **2009**, *87*, 1067.
- (40) Hui, S. W.; Viswanathan, R.; Zasadzinski, J. A.; Israelachvili, J. N. *Biophys. J.* **1995**, *68*, 171.
- (41) Jensen, M. O.; Mouritsen, O. G. *Biochim. Biophys. Acta* **2004**, *1666*, 205.
- (42) Lehtonen, J. Y. A.; Kinnunen, P. K. J. *Biophys. J.* **1984**, *46*, 141.
- (43) Dumas, F.; Tocanne, J. F.; Leblanc, G.; Lebrun, M. C. *Biochemistry* **2000**, *39*, 4846.
- (44) Merino, S.; Domènech, O.; Viñas, M.; Montero, M. T.; Hernández-Borrell, J. *Langmuir* **2005**, *21*, 4642.
- (45) Olilla, S.; Hyvonen, M. T.; Vattulainen, I. *J. Phys. Chem. B* **2007**, *111*, 3139.
- (46) Seeger, H. K.; Bortolotti, C. A.; Alessandrini, A.; Facci, P. *J. Phys. Chem. B* **2009**, *113*, 16654.
- (47) Picas, L.; Merino-Montero, S.; Morros, A.; Hernández-Borrell, J.; Montero, M. T. *J. Fluoresc.* **2007**, *17*, 649.